Journal of Innovations in Engineering Education
JIEE 2025, Vol. 8, Issue 1.

https://doi.org/10.3126/jiee.v8i1.87191

THAPATHALI CAMPUS
Institute of Engineering
Tribhuvan University

Free vibration analysis of an Air Compressor Blade by using Euler Bernoulli and Timoshenko Beam theory

Rajiv Kumar Khadka[a], Hari Bishal Koirala[a] and Bikki Chhantyal[a,*]

[a]*Department of Automobile and Mechanical Engineering, Thapathali Campus, Tribhuvan University, Kathmandu, Nepal*

ARTICLE INFO

Article history:

Received 30 July 2025
Revised in 9 December 2025
Accepted 23 December 2025

Keywords:

Resonant vibrations
Shear deformation
Rotary inertia
Euler Bernoulli beam
Timoshenko beam

Abstract

Compressor blades in gas turbines are highly susceptible to resonant vibrations caused by aerodynamic and mechanical loads, which can lead to fatigue failure. Accurate prediction of their natural frequencies is crucial to ensure safe and efficient operation. This study investigates the free vibration characteristics of a compressor blade with a NACA 6412 airfoil cross-section using both analytical and numerical methods. The blade was modeled as a cantilever beam, and natural frequencies were calculated using Euler-Bernoulli and Timoshenko beam theories. While the Euler-Bernoulli theory neglects shear deformation and rotary inertia, the Timoshenko theory includes both, making it more suitable for thicker or moderately short blades. Material and geometric properties of the blade were incorporated to compute the first three modal frequencies. To validate the analytical results, a 3D finite element model of the blade was developed in ANSYS, and modal analysis was performed under fixed-root conditions. The comparison revealed that both beam theories closely matched the FEM result for the first natural frequency. However, at higher modes, Timoshenko theory demonstrated greater accuracy than Euler-Bernoulli by accounting for shear and rotary effects.

1. Introduction

The compressor blades in gas turbines are subjected to complex dynamic loads arising from aerodynamic forces, mechanical imbalances, and operational wear, which can cause resonant vibrations, fatigue, and catastrophic failure [1, 2]. Aerodynamic excitation, caused by unsteady flow interactions between the rotor and stator blades, induces oscillatory pressures that excite the natural frequencies of the blade [1, 3]. These vibrations are further exacerbated by mechanical imbalances due to manufacturing tolerances or degradation in service, such as erosion or foreign object damage (FOD), which alter the mass distribution and stiffness of the blade [4, 5]. For instance, [5] demonstrated that a 5% thickness reduction from erosion can increase the natural frequency of first mode by 8%, while FOD significantly modifies mode shapes and stress distributions [6, 7]. While classical beam theories like Euler-Bernoulli and Timoshenko Beam Theory are widely used to model blade dynamics, their applicability to airfoil-shaped geometries characterized by camber, thickness variations, and asymmetric stiffness remains underexplored [8, 9].

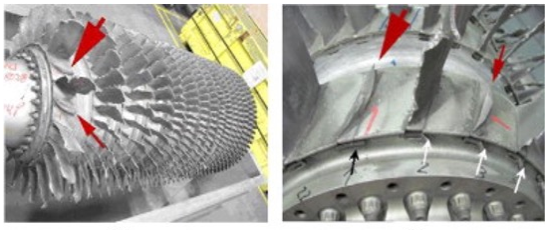

Figure 1: Fatigue Fracture of compressor blade due to aerodynamic load a) Overall view b) first state compressor

Existing studies on turbomachinery blade vibrations have predominantly focused on simplified rectangular or tapered beams, neglecting the aerodynamic-

*Corresponding author:
chhantyalbikki@tcioe.edu.np (B. Chhantyal)

structural coupling inherent to airfoils [10, 11]. For example, Srinivasan [12] experimentally validated Euler Bernoulli theory for straight blades but highlighted discrepancies in twisted or cambered profiles due to shear deformation. Similarly, Lane [3] demonstrated that the mode shapes of the system in compressor blades deviate significantly from the predictions of the classical beam in higher modes, underscoring the need for advanced models. Recent computational studies using ANSYS [13] have improved accuracy but lack theoretical validation against Timoshenko's framework for airfoils.

The NACA 6412 airfoil, with its 6% camber and 12% thickness, introduces unique challenges. Its asymmetric geometry complicates the calculation of bending inertia (I) and neutral axis position (z), which are critical for accurate modal analysis [8]. While Euler Bernoulli theory assumes negligible shear deformation which is valid for slender beams, it overestimates natural frequencies for thicker sections or higher modes, where rotary inertia and shear effects dominate [14]. Timoshenko Beam Theory addresses these limitations, but requires precise shear correction factors [15], which are rarely calibrated for airfoils.

2. Theoretical Formulations

2.1. Euler Bernoulli Beam Theory

The Euler-Bernoulli beam theory, derived from the classical work of Jacob Bernoulli and Leonhard Euler, is a foundational model for analyzing slender beams undergoing bending vibrations [14, 16]. It operates under the Kirchhoff hypothesis, which assumes:

a. The plane sections remain plane and perpendicular to the neutral axis during deformation (neglecting shear distortion).

b. The rotary inertia is negligible, which is valid for low frequency vibrations.

c. Small deformations, ensuring linear elastic material behavior.

The Euler Bernoulli theory models bending vibrations by assuming that plane sections remain plane and perpendicular to the neutral axis, neglecting shear deformation and rotary inertia. The governing equation for free vibration is:

$$EI\frac{\partial^4 y}{\partial x^4} + \rho A\frac{\partial^2 y}{\partial t^2} = 0 \tag{1}$$

where E, I, ρ and A are Young's modulus, moment of inertia area, density, and cross-sectional area, respectively. For a cantilever beam, boundary conditions are:

Figure 2: Uniform Cantilever Model

For fixed end,

$$y(0) = 0, y'(0) = 0 \tag{2}$$

For free end,

$$y''(L) = 0, y'''(L) = 0 \tag{3}$$

The frequency equation is the following.

$$\cos\beta L \cosh\beta L + 1 = 0 \tag{4}$$

To solve this equation for $\beta_n L$, which represents the eigenvalues times the length, numerical computation is performed to get,

$\beta_1 L = 1.8751, \beta_2 L = 4.6941, \beta_3 L = 7.8548, \beta_4 L = 10.9955$

$$\omega_n = \frac{(\beta_n L)^2}{L^2}\sqrt{\frac{EI}{\rho A}} \tag{5}$$

Although Euler Bernoulli theory is computationally efficient, its assumption of negligible shear deformation limits accuracy for short or thick beams and higher frequency modes where shear effects dominate [17, 18]. For instance, Levinson [17] demonstrated that Euler Bernoulli underestimates displacements by up to 30% in thick beams due to ignored shear strain energy.

2.2. Timoshenko Beam Theory

Timoshenko beam theory, developed by Stephen Timoshenko [14] extends Euler Bernoulli theory by incorporating shear deformation and rotary inertia, critical for high-frequency vibrations and stocky beams [19, 15]. The Timoshenko beam theory overrides the Kirchhoff hypothesis by accounting for shear-induced cross-sectional rotations distinct from neutral axis deformation.

The coupled PDEs are derived from force and moment equilibrium:

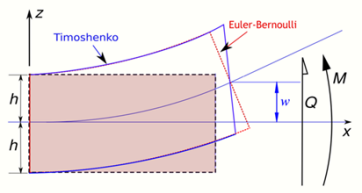

Figure 3: Bending deformation of Euler Bernoulli and Timoshenko Beam

beginequation $-\frac{\partial Q(x,t)}{\partial x} + \rho A \frac{\partial^2 y(x,t)}{\partial t^2} = 0$

$$-\frac{\partial M(x,t)}{\partial x} + Q(x,t) - I\rho\frac{\partial^2\theta}{\partial t^2} = 0 \tag{6}$$

where, $Q(x,t) = kGA\gamma(x,t)$

$M(x,t) = EI\frac{\partial\theta(x,t)}{\partial x}$

k is the shear correction factor (0.85–0.9 for solid sections; [15].

Using the separation of variable

$$y(x,t) = X(x)T(t); \theta(x,t) = Y(x)T(t) \tag{7}$$

Equations 6 and 7 become

$$X''(x) + aX(x) - Y'(x) = 0 \tag{8}$$

$$Y''(x) + bY(x) + c(x) = 0 \tag{9}$$

$$\ddot{T} + \omega^2 T(t) = 0 \tag{10}$$

Where,

$a = \frac{\omega^2\rho}{kG}, b = \frac{\omega^2\rho}{E} - c, c = \frac{GkA}{EI}$

Putting value of $Y''(x)$ from equation 9 in equation 8,

$$X''''(x) + dX''(x) + eX(x) = 0 \tag{11}$$

Where,

$d = a + b + c$ and $e = ab$

Also, $\Delta = d^2 - 4e$ and $\lambda_1 = \frac{1}{2}(-d + \sqrt{\Delta}), \lambda_1 = \frac{1}{2}(-d - \sqrt{\Delta})$

Boundary conditions for the cantilever beam are:

at $x = 0, X(0) = 0$ and $X'''(0) + (a + c)X'(0) = 0$

at $x = L, dX'(L) + X'''(L) = 0$ and $X''(L) + aX(L) = 0$

For $\omega = \sqrt{\frac{GkA}{\rho I}}$

Natural frequencies of the beam are determined from the equation: $|A| = 0$. where,

$$A = \begin{bmatrix} 1 & 0 & 1 & 0 \\ 0 & a_{22} & 0 & a_{24} \\ a_{31} & a_{32} & a_{33} & a_{34} \\ a_{41} & a_{42} & a_{43} & a_{44} \end{bmatrix}$$

$a_{22} = \lambda_1(\lambda_1^2 + a + c)$

$a_{24} = \lambda_2(-\lambda_2^2 + a + c)$

$a_{31} = (\lambda_1^2 - d)\lambda_1 \sinh\lambda_1 L$

$a_{32} = (\lambda_1^2 - d)\lambda_1 \cosh\lambda_1 L$

$a_{33} = (\lambda_2^2 + d)\lambda_2 \sin\lambda_2 L$

$a_{34} = (-\lambda_2^2 - d)\lambda_2 \cos\lambda_2 L$

$a_{41} = (\lambda_1^2 + a)\cosh\lambda_1 L$

$a_{42} = (\lambda_1^2 + a)\sinh\lambda_1 L$

$a_{43} = (-\lambda_2^2 + a)\cos\lambda_2 L$

$a_{44} = (-\lambda_2^2 + a)\sin\lambda_1 L$

Timoshenko Beam Theory's accuracy hinges on k, which accounts for non-uniform shear stress distribution. For airfoils, k is derived from cross-sectional geometry [15, 20].

2.2.1. Finite Element Validation

Finite element methods (FEM) resolves limitations of analytical beam theories [21, 22] by discretizing complex geometries. ANSYS Workbench employs hexahedral elements with shape functions approximating displacements and rotations, minimizing shear locking [13].

3. Area and Bending Inertia of Airfoil section

3.1. Airfoil Data

For the cross section of blade geometry, NACA6412 airfoil is chosen. This NACA airfoil series is controlled by 4 digits e.g. NACA 2412, which designate the camber, position of the maximum camber and thickness. If an airfoil number is NACA MPXX. e.g.

NACA 6412 then:

M is the maximum camber divided by 100. In the example M=6 so the camber is 0.06 or 6% of the chord

P is the position of the maximum camber divided by 10. In the example P=4 so the maximum camber is at 0.4 or 40% of the chord.

XX is the thickness divided by 100. In the example XX=12 so the thickness is 0.12 or 12% of the chord.

3.2. Area and Bending Inertia

As described in section 2.1 and 2.2, calculation of the natural frequency of a blade requires knowing the spanwise bending stiffness distribution $EI(y)$ along the primary axis of loading. For a wing made of a uniform solid material, the modulus E is the modulus of elasticity of material. The moment of inertia $I(y)$ of the airfoil cross-sections about the bending axis x (called the bending inertia), is then related only to the airfoil shape given by the upper and lower surfaces $Z_u(x)$ and $Z_l(x)$. As shown in Figure 5, both the area A and the total bending inertia I are the integrated contributions of all the infinitesimal rectangular sections, each dx wide and $Z_u(x) - Z_l(x)$ tall. The inertia of each such section is appropriately taken about the neutral surface position z defined for the entire cross section.

These relations assume that the bending deflection will occur in the z direction, which is a good assumption if the x axis is parallel to the airfoil's chord line.

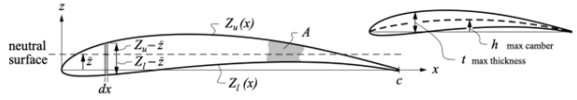

Figure 4: Upper curve, Lower curve and neutral surface of Airfoil

$$\text{Area, } A = \int_0^c (Z_u - Z_l)dx$$

$$\text{Neutral axis, } \bar{z} = \frac{1}{2A}\int_0^c (Z_u^2 - Z_l^2)dx$$

$$\text{Moment of inertia, } I = \frac{1}{3}\int_0^c ((Z_u - \bar{z})^3 - (Z_l - \bar{z}))^3 dx$$

4. Modal Analysis using ANSYS

In order to predict the dynamic behavior of the structure properly via forming FEM, the model should be validated by tests. In the validation process, obtained test data were used for comparison with the predicted data obtained by FEM. If the model is incapable of predicting the dynamic properties of the structure accurately, it has to include some useful information about the dynamic properties of the structure. In the study of Bagul et al., the confirmation has been performed by using ANSYS Workbench.

4.1. Geometry

The compressor blade considered for the analysis has been taken from literature [23, 24]. Depending upon the operation condition and compressor stage, the compressor section considered being high-pressure compressor section design parameters were laid out in design conditions [23]. A compressor rotor assembly has been designed based on those parameters for a compressor design overview [24]. Since a compressor rotor assembly is a complex assembly with multiple degrees of freedom and large variables [25], a single blade design is made to carry out vibrational study. The disk is taken to be a pre-twisted compressor blade with a fir-tree root type, designed to simplify analysis [26]. A CAD model of the compressor disk and single blade is represented in the figure below.

The modeled structure was an aircraft wing of airfoil cross-section NACA 6412 series with steel [8, 27]. The chord length of the airfoil is 0.1 m, and the wing length is 0.15 m.

The compressor blade considered for the analysis has been taken from literature. Depending upon the operation condition and compressor stage the compressor section considered being high pressure compressor section design parameters were laid out in design conditions. A compressor rotor assembly has been designed based on those parameters for a compressor design overview. Since a compressor rotor assembly is a complex assembly with multiple degrees of freedom and large variables, a single blade design is made to carry out vibrational study. The disk is taken to be a pre-twisted compressor blade with fir tree root type has been designed to make analysis simpler. CAD model of compressor disk and single blade is represented in the figure below.

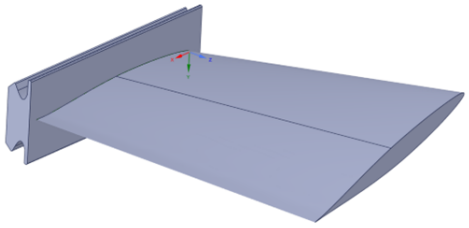

Figure 5: CAD Model of twisted blade with fir tree root

The modeled structure was an aircraft wing of airfoil cross section NACA 6412 series with Steel. The chord length of the airfoil is 0.1 m and wing length is 0.15 m.

4.2. Meshing

The structured meshing was done in blade using sweep method. One airfoil section is selected as source and

other as target. The number of divisions was put to be 50. For simplicity, the root of the blade was removed. The meshing was started with body sizing of 8 mm. The sizing was reduced to 4 mm, 2 mm finally to 1 mm for grid convergence study.

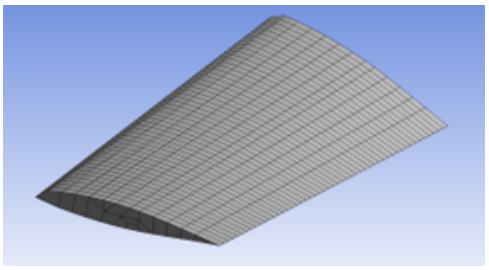

Figure 6: Hexahedral Meshing of 8 mm mesh size

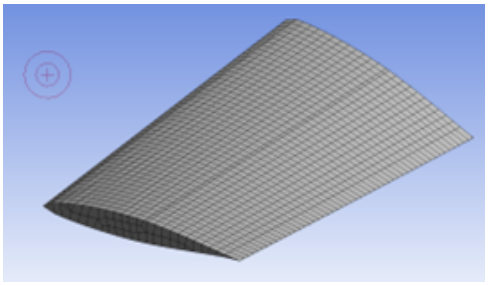

Figure 7: Hexahedral Meshing of 4 mm mesh size

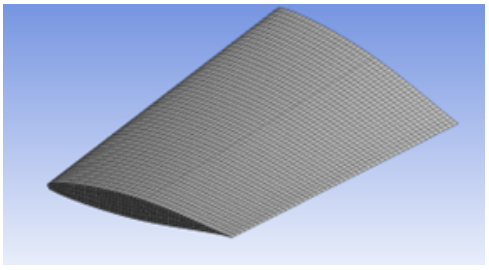

Figure 8: Hexahedral Meshing of 2 mm mesh size

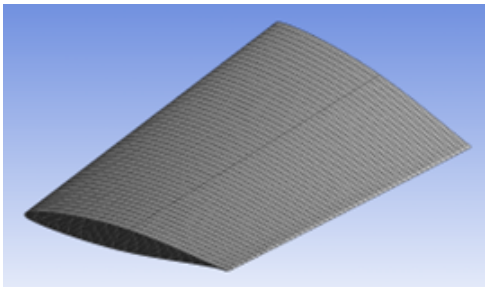

Figure 9: Hexahedral Meshing of 1 mm mesh size

4.2.1. Grid Convergence Study

The details of the mesh for different sizes are in the Table 1.

Table 1: First Natural Frequency at Various Modes

S.N.	Nodes	Elements	Natural Freq. (Hz)
1	1581	950	303.2
2	3672	2450	301
3	12291	9600	299.87
4	40800	35050	299.69

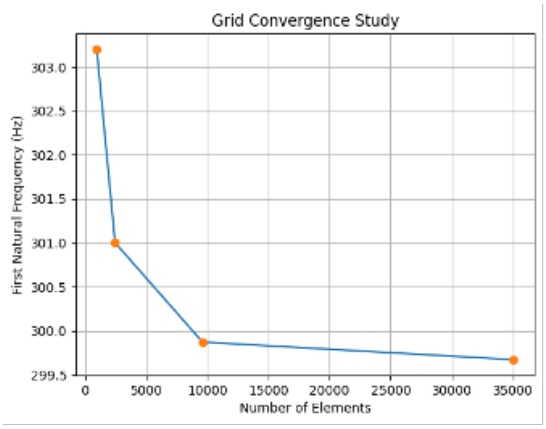

Figure 10: Grid Convergence Study, First natural frequency vs No. of elements

4.3. Simulation Setup and Boundary Conditions

The blade is considered a cantilever beam. One end of the blade is given fixed support and the other is kept free.

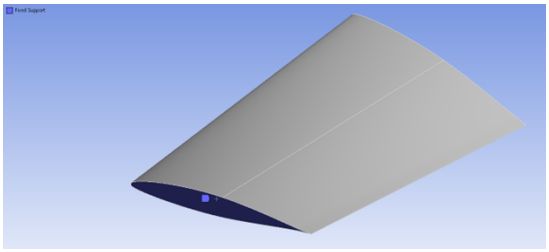

Figure 11: Boundary Conditions showing one end of cross section fixed and other end free

4.4. Natural frequencies and Mode shapes

The natural frequencies obtained from fem analysis using ANSYS is as follows in Table 2.

Table 2: Natural Frequency at various modes

Mode	Natural Frequency (Hz)
1	299.87
2	1688.3
3	4607.8
4	7807

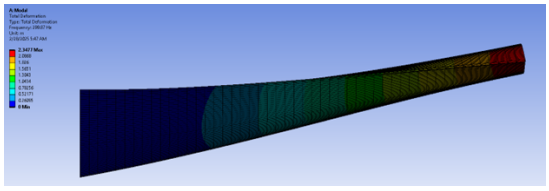

Figure 12: First mode bending vibration

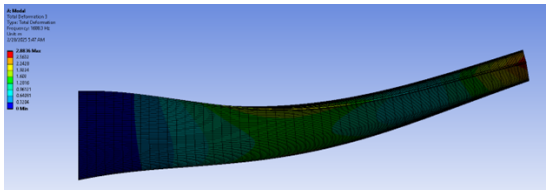

Figure 13: Second mode bending vibration

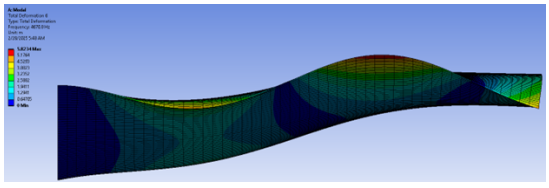

Figure 14: Third mode bending vibration

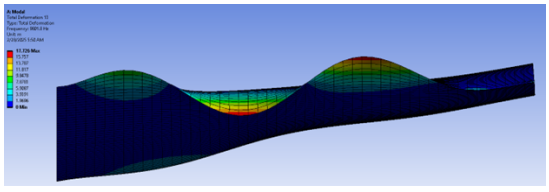

Figure 15: Fourth mode bending vibration

5. Results and Discussion

5.1. Euler Bernoulli

By using formula of section 3.2.

Area of blade, A = $687.2 \times 10^{-6} m^2$

Moment of inertia of blade, $I = 3760 \times 10^{-12} m^4$

The Natural frequency using Euler Bernoulli beam model is shown in Table 3.

Table 3: Natural frequency using Euler Bernoulli

Mode No.	Natural Frequency (Hz)
1	293.6
2	1840.58
3	5153.73
4	10099.08

5.2. Timoshenko

The Natural frequency using Natural frequency using Timoshenko beam model is shown in Table 4.

Table 4: Natural frequency using Timoshenko

Mode No.	Natural Frequency (Hz)
1	294.82
2	1847.73
3	5093.03
4	9732.08

5.3. FEM Using ANSYS

The Natural frequency using ANSYS is shown in Table 5.

Table 5: Natural frequency using ANSYS

Mode No.	Natural Frequency (Hz)
1	299.87
2	1688.3
3	4670.8
4	9801.8

The results of the free vibration analysis using Euler-Bernoulli beam theory, Timoshenko beam theory, and ANSYS simulations reveal critical insights into the dynamic behavior of the NACA 6412 airfoil compressor blade.

Comparison of Natural Frequencies First Mode: The theoretical Euler Bernoulli (293.6 Hz) and Timoshenko Beam Theory (294.82 Hz) predictions align closely with ANSYS (299.87 Hz), with a slight discrepancy (2% error). This validates the applicability of both beam theories for fundamental mode analysis of slender blades. The minor difference between two theories here indicates negligible shear deformation effects in low-frequency regimes.

Higher Modes: Significant deviations emerge in the second and third modes. For instance, ANSYS predicts a second-mode frequency of 1688.3 Hz, markedly lower than Euler Bernoulli (1840.58 Hz) and Timoshenko Beam Theory (1847.73 Hz). This divergence

likely stems from geometric complexities (e.g., camber, thickness variations) and 3D effects in the airfoil, which are simplified in 1D beam theories. Timoshenko Beam Theory's closer agreement with ANSYS in the fourth mode (9732.08 Hz vs. 9801.8 Hz) highlights its superiority in modeling high-frequency vibrations where shear deformation and rotary inertia become critical. The NACA 6412 airfoil's 6% camber and 12% thickness introduce asymmetric bending and localized stiffness variations, which beam theories approximate as uniform cross-sections. This simplification explains the overestimation of frequencies by Euler Bernoulli and Timoshenko Beam Theory in higher modes. ANSYS, which accounts for the actual airfoil profile, captures these nuances, resulting in lower frequencies (e.g., 4670.8 Hz vs. 5153.73 Hz in Mode 3).

The mesh convergence study confirmed mesh independence, with the first natural frequency stabilizing at $\tilde{2}$99.69 Hz for a 1mm mesh. This ensures the reliability of ANSYS results. The close match between Timoshenko Beam and ANSYS in higher modes (e.g., Mode 4) underscores the importance of refining theoretical models to include shear effects for thick or short blades.

6. Conclusions

In this study, the Euler-Bernoulli and Timoshenko beam theory was compared with ANSYS simulations to analyze the free vibration characteristics of a NACA 6412 airfoil compressor blade. The results highlight key trade-offs between simplicity and accuracy in modeling blade dynamics. For low-frequency vibrations (e.g., first mode), both Euler Bernoulli and Timoshenko Beam align closely with ANSYS results (2% error), validating their utility for slender blade analysis. However, higher modes reveal significant deviations, with Euler Bernoulli and Timoshenko Beam Theory overestimating frequencies by up to 10% compared to ANSYS. These discrepancies stem from the geometric complexities of the airfoil, such as camber and thickness variations, which beam theories simplify as uniform cross sections. Timoshenko Beam Theory's closer agreement with ANSYS in the fourth mode (0.7% error) underscores its advantage in capturing shear and rotary inertia effects critical for high-frequency regimes.

Acknowledgments

The authors are grateful to Department of Automobile and Mechanical Engineering, Thapathali Campus for neccesary support to complete this article.

References

[1] Carta F O. An analysis of stator blade vibration due to rotor/stator interaction[J/OL]. J. Eng. Gas Turbines Power, 1982, 104(1): 129-136. DOI: 10.1115/1.3240815.

[2] Griffin J H. Friction damping of resonant stresses in gas turbine engine airfoils[J/OL]. J. Eng. Power, 1980, 102(2): 329-333. DOI: 10.1115/1.3224779.

[3] Lane F. System mode shapes in the flutter of compressor blade rows[J/OL]. J. Aeronaut. Sci., 1956, 23(1): 54-62. DOI: 10.2514/8.3650.

[4] Muszyńska A. Rotordynamics[M]. Boca Raton, FL: CRC Press, 2005.

[5] Hamed A, Tabakoff W, Wenglarz R. Turbine blade surface deterioration by erosion[J/OL]. J. Turbomach., 2006, 128(3): 445-452. DOI: 10.1115/1.2204629.

[6] Legrand M, Jardine A P, Gallardo C A. Foreign object damage in gas turbine blades[J/OL]. Eng. Fail. Anal., 2012, 25: 1-10. DOI: 10.1016/j.engfailanal.2011.11.001.

[7] Tabakoff W, Hamed A, Metwally M. Erosion effects on turbomachinery performance[J/OL]. J. Fluids Eng., 1990, 112(1): 88-94. DOI: 10.1115/1.2909384.

[8] Abbott I H, Doenhoff A E V. Theory of wing sections[M]. New York: Dover, 1959.

[9] Bisplinghoff R L, Ashley H, Halfman R L. Aeroelasticity[M]. Cambridge, MA: Addison-Wesley, 1996.

[10] Kielb R E, Korta J J, Srinivasan A V. Flutter of turbomachinery blades and disks[J/OL]. AIAA J., 2003, 41(10): 1927-1934. DOI: 10.2514/2.6854.

[11] Marshall J G, Imregun M. Blade vibration in axial turbomachines[J/OL]. J. Sound Vib., 2003, 259(1): 241-256. DOI: 10.1006/jsvi.2002.5157.

[12] Srinivasan A V. Flutter and resonant vibration characteristics of engine blades[J/OL]. J. Eng. Gas Turbines Power, 1997, 119 (4): 742-775. DOI: 10.1115/1.2817050.

[13] Bagul Y D, Ranaware V V, Patil S R. Modal analysis of gas turbine blade using ansys[J/OL]. IOP Conf. Ser.: Mater. Sci. Eng., 2017, 225: 012009. DOI: 10.1088/1757-899X/225/1/012009.

[14] Timoshenko S P. On the correction for shear of the differential equation for transverse vibrations of prismatic bars[J/OL]. Philos. Mag., 1921, 41: 744-746. DOI: 10.1080/14786442108636264.

[15] Cowper G R. The shear coefficient in timoshenko's beam theory[J/OL]. J. Appl. Mech., 1966, 33: 335-340. DOI: 10.1115/1.3569049.

[16] Reddy J N. A simple higher-order theory for laminated composite plates[J/OL]. J. Appl. Mech., 1984, 51: 745-752. DOI: 10.1115/1.3167719.

[17] Levinson M. A new rectangular beam theory[J/OL]. J. Sound Vib., 1981, 74(1): 81-87. DOI: 10.1016/0022-460X(81/90193-9.

[18] Stephen N G. Timoshenko's shear coefficient from a beam subjected to gravity loading[J/OL]. J. Sound Vib., 1981, 77(1): 103-109. DOI: 10.1016/0022-460X(81/90310-1.

[19] Timoshenko S P. On the transverse vibrations of bars of uniform cross-section[J/OL]. Philosophical Magazine, 1922, 43(253): 125-131. DOI: 10.1080/14786442208633870.

[20] Hutchinson J R. Shear coefficients for timoshenko beam theory[J/OL]. J. Appl. Mech., 2001, 68: 87-92. DOI: 10.1115/1.1370373.

[21] Bathe K J. Finite element procedures[M]. Englewood Cliffs, NJ: Prentice-Hall, 1996.

[22] Zienkiewicz O C, Taylor R L, Zhu J Z. The finite element method: Its basis and fundamentals[M]. 6th ed. Oxford: Butterworth-Heinemann, 2005.

[23] Cumpsty N A. Compressor aerodynamics[M]. Melbourne, FL: Krieger Publishing, 2004.

[24] Casey M V. Centrifugal compressors: A strategy for aerodynamic design and analysis[J/OL]. ASME J. Turbomach., 2000, 122(3): 357-365. DOI: 10.1115/1.1303075.
[25] Carta F O. Coupled blade-disk-shroud flutter in turbomachines[J/OL]. J. Propuls. Power, 1987, 3(2): 165-171. DOI: 10.2514/3.22964.
[26] Manwaring S R, Kirkegaard K C. Blade root attachment vibration characteristics in turbomachinery[J/OL]. ASME J. Eng. Gas Turbines Power, 1997, 119(2): 345-352. DOI: 10.1115/1.2815586.
[27] Sinha S K. Dynamic characteristics of a timoshenko beam using fem[J/OL]. J. Sound Vib., 2006, 291(1–2): 372-386. DOI: 10.1016/j.jsv.2005.06.007.